The effect of halogenation on PBDTT-TQxT based non-fullerene polymer solar cells - Chlorination vs fluorination

Peer-reviewed author version

LENAERTS, Ruben; DEVISSCHER, Dries; PIROTTE, Geert; GIELEN, Sam; MERTENS, Sigurd; CARDEYNAELS, Tom; Champagne, Benoit; LUTSEN, Laurence; VANDERZANDE, Dirk; ADRIAENSENS, Peter; VERSTAPPEN, Pieter; VANDEWAL, Koen & MAES, Wouter (2020) The effect of halogenation on PBDTT-TQxT based non-fullerene polymer solar cells - Chlorination vs fluorination. In: Dyes and Pigments, 181 (Art N° 108577).

DOI: 10.1016/j.dyepig.2020.108577
Handle: http://hdl.handle.net/1942/31936

The effect of halogenation on PBDTT-TQxT based non-fullerene polymer solar cells – chlorination vs fluorination

Ruben Lenaerts[#,1,2] Dries Devisscher[#,1,2] Geert Pirotte,[1,2] Sam Gielen,[1,2] Sigurd Mertens,[1,2] Tom Cardeynaels,[1,2,3] Benoît Champagne,[3] Laurence Lutsen,[2] Dirk Vanderzande,[1,2] Peter Adriaensens,[1,2] Pieter Verstappen,[1,2] Koen Vandewal,[1,2] Wouter Maes[1,2]*

[#] These authors contributed equally to this work.

[1] UHasselt – Hasselt University, Institute for Materials Research (IMO-IMOMEC), Agoralaan 1, 3590 Diepenbeek, Belgium

[2] IMOMEC Division, IMEC, Wetenschapspark 1, 3590 Diepenbeek, Belgium

[3] University of Namur, Laboratory of Theoretical Chemistry, Theoretical and Structural Physical Chemistry Unit, Namur Institute of Structured Matter, Rue de Bruxelles 61, 5000 Namur, Belgium

Abstract

The rapid advancement in the development of non-fullerene acceptors has led to single-junction polymer solar cells with efficiencies over 18%. Even with these novel acceptor materials, the choice of the donor polymer remains important. Tuning of the donor and acceptor compatibility in terms of absorption, frontier orbital energy levels, mixing enthalpy and charge carrier mobility is routinely performed by side chain variation. Fluorination presents an additional powerful approach to optimize these parameters. Although significantly less studied, chlorination can give rise to similar effects, while donor-acceptor phase separation due to fluorophobic interactions is less of an issue. Moreover, from a material synthesis point of view, the introduction of chlorine groups is in many cases much more straightforward. In this work, we present a series of push-pull type benzo[1,2-*b*:4,5-*b*']dithiophene-*alt*-quinoxaline donor polymers and compare the behavior of the non-halogenated, fluorinated and chlorinated derivatives in polymer solar cells when combined with small molecule and polymer type non-fullerene acceptors. The solar cell efficiencies vary from 2.4 to 8.4%, elucidating the large impact of these small structural variations. Best results are achieved for the chlorinated donor polymer, affording a high open-circuit voltage, balanced charge carrier mobilities and favorable donor-acceptor interactions. Combined with the easier synthesis of chlorinated materials, this suggests that more emphasis should be put on chlorination as a valuable approach to tune the properties of organic semiconductors for solar cell blends (and other optoelectronic applications).

Keywords

organic photovoltaics; fullerene-free; all-polymer; chlorination; fluorination

Introduction

In recent years, non-fullerene acceptors (NFAs) have been established as a better alternative for traditional fullerene derivatives in bulk heterojunction organic photovoltaics (OPVs),[1-9] addressing particular shortcomings in terms of light absorption, energy losses and production costs.[6,10-13] Power conversion efficiencies (PCEs) over 18% have now been realized with small molecule acceptors in single-junction devices.[1,14] All-polymer solar cells lag a bit behind in efficiency, with PCEs now over 11%,[2,9,15-17] but may have specific advantages with respect to ink formulation, long-term (thermal and mechanical) stability and flexibility.[8,18,19]

For these novel electron acceptors, the nature of the donor polymer obviously remains important. Among the high optical gap push-pull type copolymers affording best solar cell efficiencies in combination with NFAs, the family based on the electron-rich benzo[1,2-*b*:4,5-*b*']dithiophene (BDT) fused ring system has been very popular.[20] BDT can be readily synthesized and its rigid and planar structure with a highly delocalized π-system reduces the optical gap and favors hole transport.[21] It has also been demonstrated that appending conjugated side chains on the BDT core (e.g. alkylthienyl groups) increases the tendency to form crystallites with the desired face-on orientation. Additionally, the stabilization of the extended conjugated system lowers the highest occupied molecular orbital (HOMO) energy level, leading to an increase in the open-circuit voltage (V_{OC}).[22,23] On the other hand, the electron-deficient quinoxaline (Qx) monomer and its derivatives have also received much interest for the construction of electron donor polymers as well as non-fullerene acceptors.[24-26] The easily modifiable structure allows fine-tuning of the opto-electronic properties through the facile introduction of substituents.[27,28] This can often be done through simple, high-yielding and cheap synthetic procedures. The appealing characteristics of both BDT and Qx monomers have led to many different OPV materials affording high device efficiencies.[20,27] They are usually linked via thiophene π-spacers to prevent twisting of the backbone, which limits the conjugation length.

An often applied tool to tune the electrochemical and optical properties of active layer OPV materials is fluorination.[28-33] The introduction of fluorine atoms on organic semiconductors generally increases their thermal and chemical stability, absorption coefficient and charge carrier mobility. Moreover, through the stabilization of both frontier orbital energy levels of a fluorinated electron donor polymer, the V_{OC} can be increased while leaving the optical gap untouched. The increased planarization and

intramolecular interactions induced by the presence of fluorine atoms also promote π-π stacking, enhancing backbone ordering and crystallinity, which often has a beneficial effect on film morphology, and hence short-circuit current density (J_{SC}) and fill factor (FF). More recently, it has been demonstrated that similar positive effects can also be achieved by chlorination instead of fluorination, which has economic benefits.[34-37] Chlorinated aromatic compounds are in general more readily available. The introduction of a chlorine atom often requires fewer synthetic steps and a less tedious purification procedure as compared to introducing fluorine. However, the steric hindrance due to the larger radius of the chlorine atom can lead to (stronger) twisting of the polymer backbone, negatively impacting the photovoltaic characteristics.[38]

In 2012, fluorination of BDT-Qx donor polymer materials enabled Chen *et al. to* achieve a PCE of 8.0%, through a combination of the standard 2-ethylhexyloxy-substituted BDT and a difluorinated Qx with *m*-hexyloxyphenyl substituents, linked through a thiophene spacer.[39] Combined with $PC_{71}BM$, this polymer afforded a very high J_{SC} of 18.2 mA/cm², attributed to its broad absorption and high hole mobility. While studying the impact of fluorination on the BDT-Qx polymer, Liu and co-workers observed a clear improvement in V_{OC}.[40] They managed to raise the PCE to 8.5% through monofluorination of the BDT thienyl side group and difluorination of the Qx monomer. Employing the same polymer, Zhao *et al.* achieved a PCE of 9.0% by the application of a polymeric cathode interlayer.[41] Zheng *et al.* subsequently combined this polymer with ITIC and realized a PCE of 11.3%.[42] In several studies on the fluorination of the Qx substituents, Xu *et al.* acquired a PCE of 10.5% in combination with ITIC by introduction of a monofluorinated 2-ethylhexylthiophene side chain.[43-45] Finally, Chen *et al.* recently synthesized a copolymer from an (octylthio)thiophenyl-2-yl substituted BDT and a difluorinated Qx with thiophene spacers.[46] This polymer afforded a PCE of 8.7% with o-IDTBR as acceptor and 6.7% with the polymer acceptor N2200. Despite the increasing interest in chlorination, no attempt at synthesizing a chlorinated BDT-Qx polymer has been reported to date.

Halogenation of electron acceptor materials has been intensively studied as well.[47-49] One of the most applied classes of state-of-the-art electron accepting small molecules is based on 2-(3-oxo-2,3-dihydro-1*H*-inden-1-ylidene)malononitrile, among which are ITIC and IEICO. The absorption of tetrafluorinated and tetrachlorinated ITIC (IT-4F and IT-4Cl, respectively) is red-shifted compared to ITIC. The LUMO energy level lowers from ITIC to IT-4F to IT-4Cl, while the HOMO energy level increases.[37,50] The polymer acceptor PNDI(2OD)2T, also known by its brand name N2200 (**Figure 1**), has two halogenated derivatives, PNDI(2OD)2T2F and PNDI(2OD)2T2Cl (**Figure 1**), with the fluorine or chlorine atoms

introduced on the electron rich bithiophene part. The optical gap of the polymer increases by halogenation, which is most pronounced for the chlorination. In solar cell devices with PTB7-Th, application of PNDI(2OD)2T2F led to an increase in FF and J_{sc} due to the higher crystallinity and improved electron transport of the fluorinated acceptor polymer, reaching a PCE up to 6.71%.[33] To the best of our knowledge, PNDI(2OD)2T2Cl has not yet been investigated in bulk heterojunction organic solar cells, although it has been applied in n-channel transistors.[51]

In the presented work, we describe the synthesis of three different donor copolymers based on thiophene-substituted BDT (BDTT) combined with a difluorinated Qx (**Figure 1**). To investigate the impact of halogenation, the BDT monomer was decorated with either non-halogenated, difluorinated or monochlorinated thienyl moieties. One single chlorine atom was introduced (as opposed to two fluorine atoms) to prevent severe twisting of the thienyl side chains. The three materials were then applied in bulk heterojunction OPV devices with ITIC, PNDI(2OD)2T and PNDI(2OD)2T2Cl (**Figure 1**) as acceptors. ITIC was chosen as it is the benchmark small molecule NFA,[52] whereas PNDI(2OD)2T is an established acceptor for all-polymer OPVs.[3] As the combination of halogen atoms on both the donor and acceptor materials has been demonstrated previously to improve OPV performance,[53] the chlorinated derivative of PNDI(2OD)2T was also included. As anticipated, a higher degree of halogenation led to an increase in V_{OC}, although this only resulted in an increase in the PCE in case of the chlorinated donor PBDTClT-TQxT, reaching a PCE of 8.43% in combination with ITIC. The low V_{OC} losses of the PBDT2FT-TQxT blends enabled to reach the highest V_{OC} values, up to 0.98 V with ITIC. However, this fluorinated donor polymer underperformed as compared to both the non-halogenated and the chlorinated donor with all tested acceptors due to the significantly lowered J_{SC} and FF. In combination with the non-halogenated polymer acceptor, chlorination of the donor polymer did not improve the PCE. Introduction of chlorine on both the donor and acceptor polymers (PBDTClT-TQxT and PNDI(2OD)2T2Cl, respectively) did lead to a slight improvement, with a PCE up to 4.81%. Overall, this work shows that the use of chlorinated materials provides a facile way to tune and improve the properties of polymer:small molecule and polymer:polymer organic solar cell blends.

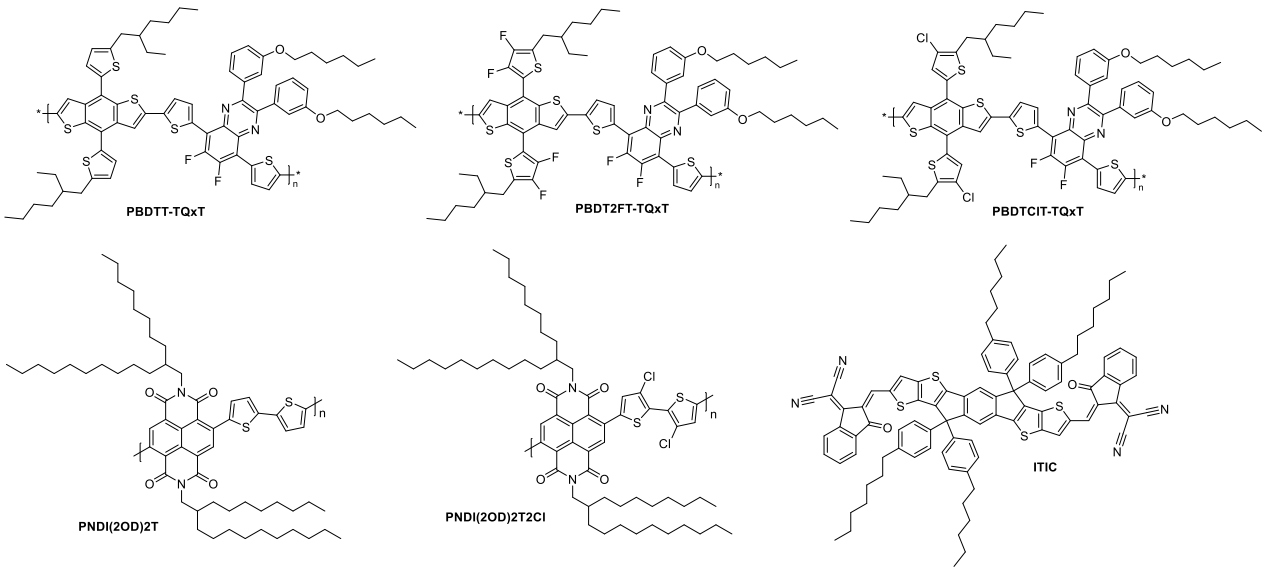

Figure 1. Chemical structures of the donor polymers PBDTT-TQxT, PBDT2FT-TQxT and PBDTClT-TQxT, and the acceptors PNDI(2OD)2T, PNDI(2OD)2T2Cl and ITIC.

Results and discussion

The synthesis procedures toward the required BDT and Qx monomers (depicted in **Scheme 1**) were taken from literature and slightly adapted.[37,39,54-57] The naphthalenediimide (NDI) and bithiophene monomers necessary for the synthesis of the acceptor polymers were also synthesized according to literature procedures.[58-60] Details on the synthetic procedures can be found in the Supplementary data.

For the halogenated BDTT monomers, the initial focus was on the difluorinated BDT2FT. During fluorination of the alkylated thiophene (step *vii* in **Scheme S1**), significant formation (>20%) of the monofluorinated derivative was observed. By taking exceptional care to avoid possible proton sources (overnight high vacuum treatment of reagents, storage of glassware in a drying oven, use of freshly dried solvents, argon atmosphere), this side reaction was inhibited. Nevertheless, the final stannylated BDT2FT contained 5-10% of the monofluorinated analogue (as analysed by ^{1}H NMR spectroscopy; **Figure S4**). Although the synthesis of this compound has been described in the past, no mention was made of the mono-F impurity and no NMR spectra were shown to confirm its absence.[54,55,61] As such, the impact of this impurity on the final OPV device performance is not known. The synthesis of the chlorinated BDTClT monomer requires significantly less steps as the chlorinated thiophene building block is commercially available and no protecting group is needed. The 'synthetic complexity' of this monomer is hence significantly smaller.[62]

All alternating copolymers were synthesized by Stille cross-coupling. The polymerizations were

performed overnight in chlorobenzene at 110 °C using the $Pd_2(dba)_3$–P(*o*-tol)$_3$ catalyst system (**Scheme 1**). Following the polymerization reactions, residual palladium traces were removed by extraction with an aqueous diethyldithiocarbamate solution, after which the polymers were separated into fractions with varying solubility (molar mass) using Soxhlet extractions. Details on the reaction conditions and work-up can be found in the Supplementary data.

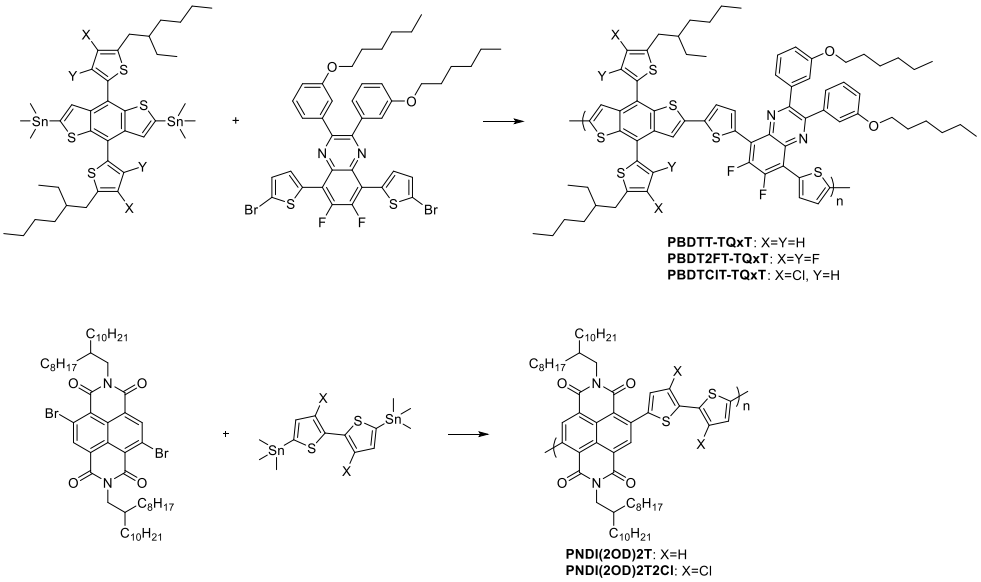

Scheme 1. Synthesis of the BDTT and NDI based copolymers by Stille cross-coupling. All polymerization reactions were performed with $Pd_2(dba)_3$ and P(*o*-tol)$_3$ in chlorobenzene at 110 °C.

The molar mass distributions of the donor and acceptor copolymers were analyzed by gel permeation chromatography (**Figure S1**), which was performed at high temperature (140 °C in *o*-dichlorobenzene) to minimize polymer aggregation. The observed values (**Table 1**) are all in the same range, which allows proper comparison of the OPV device parameters. MALDI-ToF (matrix-assisted laser desorption/ionization - time of flight) mass spectrometry was performed to analyze the structural compositions of the polymers (**Figure S10–S14**). Methyl (from the trimethylstannyl reactive groups), phenyl (from the reaction solvent), tolyl (from the phosphine ligands) and bromine end groups were detected. For PBDTT-TQxT and PBDTClT-TQxT, some minor signals pointing to homocoupled side products could be identified.[63,64]

The polymer donor materials have similar absorption patterns with a main band due to intramolecular charge transfer peaking around 600 nm and smaller bands which can be attributed to the π-π transitions of the individual building blocks (**Figure 2**). The absorption spectra of the halogenated polymers are slightly blue-shifted compared to the reference polymer PBDTT-TQxT. The optical gaps are within the

range of 1.71 to 1.79 eV (**Table 1**). Based on cyclic voltammetry (CV) measurements, the HOMO energy level for both the fluorinated and the chlorinated donor polymer are found to be around −5.55 eV, whereas the HOMO of PBDTT-TQxT is slightly higher (−5.46 eV; **Figure S2**). The LUMO energy levels remain virtually the same (−3.35 eV) (**Table 1**), as expected since the quinoxaline monomer remains unaffected. The lower HOMO levels for the halogenated donor polymers are in line with the blue-shifted absorption spectra.

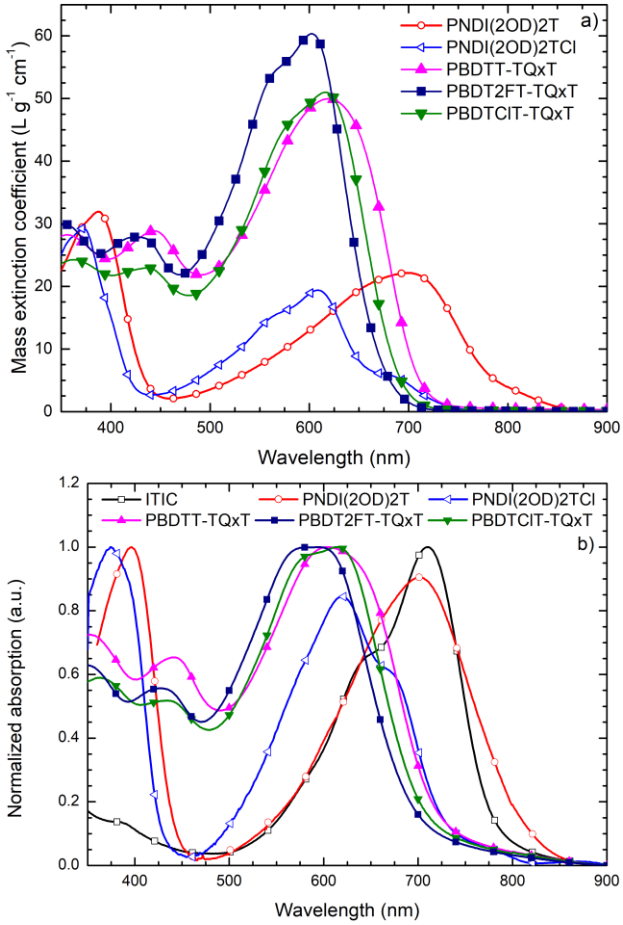

Figure 2. UV-Vis-NIR absorption spectra of the different donor and acceptor materials in solution (a) and normalized absorption spectra in thin film (b).

Table 1. Molar mass (distribution), optical and electrochemical data for the donor and acceptor materials.

	M_n (10^4 g mol^{-1})	$Đ$	HOMO[a] (eV)	LUMO[a] (eV)	E_g^{OP} [b] (eV)
PBDTT-TQxT	4.5	2.0	-5.46 (-5.34)	-3.35 (-2.69)	1.71
PBDT2FT-TQxT	5.0	2.1	-5.58 (-5.43)	-3.37 (-2.80)	1.79
PBDTClT-TQxT	7.1	1.8	-5.53 (-5.45)	-3.35 (-2.81)	1.78
PNDI(2OD)2T	4.2	2.4	-6.02 (-5.92)	-3.99 (-3.49)	1.52
PNDI(2OD)2T2Cl	5.7	2.0	-6.30 (-6.40)	-4.13 (-3.70)	1.70
ITIC	/	/	-5.80	-4.17	1.59

[a] Determined by CV from the onset of oxidation/reduction. Values from DFT calculations in parentheses (M06 exchange-correlation functional, 6-311G(d) basis set). [b] Optical gap, determined by the onset of the solid-state UV-Vis-NIR absorption spectrum.

Chlorination of the polymer acceptor PNDI(2OD)2T, yielding PNDI(2OD)2T2Cl, has a more significant impact on the absorption spectrum. The absorption spectrum of the latter is strongly blue-shifted compared to that of the former, with an optical gap in film of 1.70 eV, compared to 1.52 eV, respectively (**Table 1**, **Figure 2**). The absorption maximum of PNDI(2OD)2T2Cl is blue-shifted to ~600 nm (vs ~700 nm for PNDI(2OD)2T and 684 nm for the fluorinated analogue[65]), likely due to a combination of electronic and steric factors (*vide infra*). The small molecule acceptor ITIC has an absorption maximum in the same wavelength range as PNDI(2OD)2T, with an optical gap of 1.59 eV. Based on electrochemical analysis, PNDI(2OD)2T has the highest LUMO level (−3.99 eV), followed by PNDI(2OD)2T2Cl (−4.13 eV) and ITIC (−4.17 eV), which is hence the strongest acceptor in the series (**Figure S2**).

To achieve additional insights on the above optical and electrochemical results and to get an idea of the geometry of the BDTT-TQxT and NDI-2T copolymer structures, density functional theory (DFT) calculations were carried out using Gaussian16[66] with the M06 exchange-correlation functional[67] and the 6-311G(d) basis set. The geometries of D-A-D-A-D (D = donor, A = acceptor) type oligomers for NDI-2T and D-A-D-A oligomers for BDTT-TQxT were optimized (**Figure S15–S19**). Different conformations (with respect to the orientation of the D and A subunits) were investigated and the most stable conformers were further analyzed. For the NDI-2T oligomers, the influence of the relatively large chlorine atoms on the dihedral angle between the two thiophene units is obvious. The torsion angle between the central thiophene units enlarges from 24.4° for PNDI(2OD)2T to 46.0° for PNDI(2OD)2T2Cl. This is in line with the blue-shifted absorption for PNDI(2OD)2T2Cl as the larger twist disrupts conjugation along the polymer backbone. The HOMO is also slightly less delocalized along the oligomer backbone. For the PBDT-TQxT series, the influence of the halogen atoms is smaller because they are

found in the BDT side chains, as opposed to being in the backbone for the acceptor polymers. No apparent changes in the HOMO nor LUMO topologies can be observed as the thiophene units in the BDT side chains appear to be electronically decoupled from the BDT unit itself. However, due to the electron-deficient nature of these atoms, it is viable that they decrease the donor strength of the BDT units. The calculated HOMO-LUMO energy levels are in good (qualitative) agreement with the trends observed experimentally (Table 1).

Bulk heterojunction organic solar cells were then prepared using (mostly) the inverted device architecture glass/ITO/ZnO/active layer/MoO_x/Ag. The optimized device performance data are listed in **Table 2** and the corresponding *J*-*V* curves are depicted in **Figure 3**. All device optimization efforts can be retrieved from **Table S1–S3**. For the best devices, the donor:acceptor solutions were processed from chlorobenzene with addition of 1,8-diiodooctane (DIO) as a processing additive. With ITIC as the acceptor, PBDTT-TQxT afforded an average PCE of 7.4%.[42] When using the halogenated polymer donors (Table 2) the V_{OC} values were higher, as anticipated because of the deeper HOMO levels. Despite affording the highest V_{OC} (0.98 V) in the series, a significantly lower FF and J_{SC} were observed for the PBDT2FT-TQxT:ITIC blend, leading to the lowest average PCE of 4.9%. In the case of PBDTClT-TQxT, the J_{SC} increased and the FF remained high, affording an average PCE of 8.2%. For the all-polymer solar cells, the PBDTT-TQxT:PNDI(2OD)2T devices gave the highest PCE of 4.6%. The efficiency went down for the halogenated donor polymers PBDTClT-TQxT (3.8%) and PBDT2FT-TQxT (2.2%). Although the V_{OC} again improved upon moving from the non-halogenated to the chlorinated and fluorinated donor polymer, this effect was not sufficient to compensate the strong reduction of the J_{SC} and FF. For the all-polymer solar cells based on the chlorinated acceptor polymer PNDI(2OD)2T2Cl, the best efficiency was obtained for the chlorinated donor polymer PBDTClT-TQxT, with an average PCE of 4.3%, followed by PBDTT-TQxT (3.5%) and PBDT2FT-TQxT (2.4%).

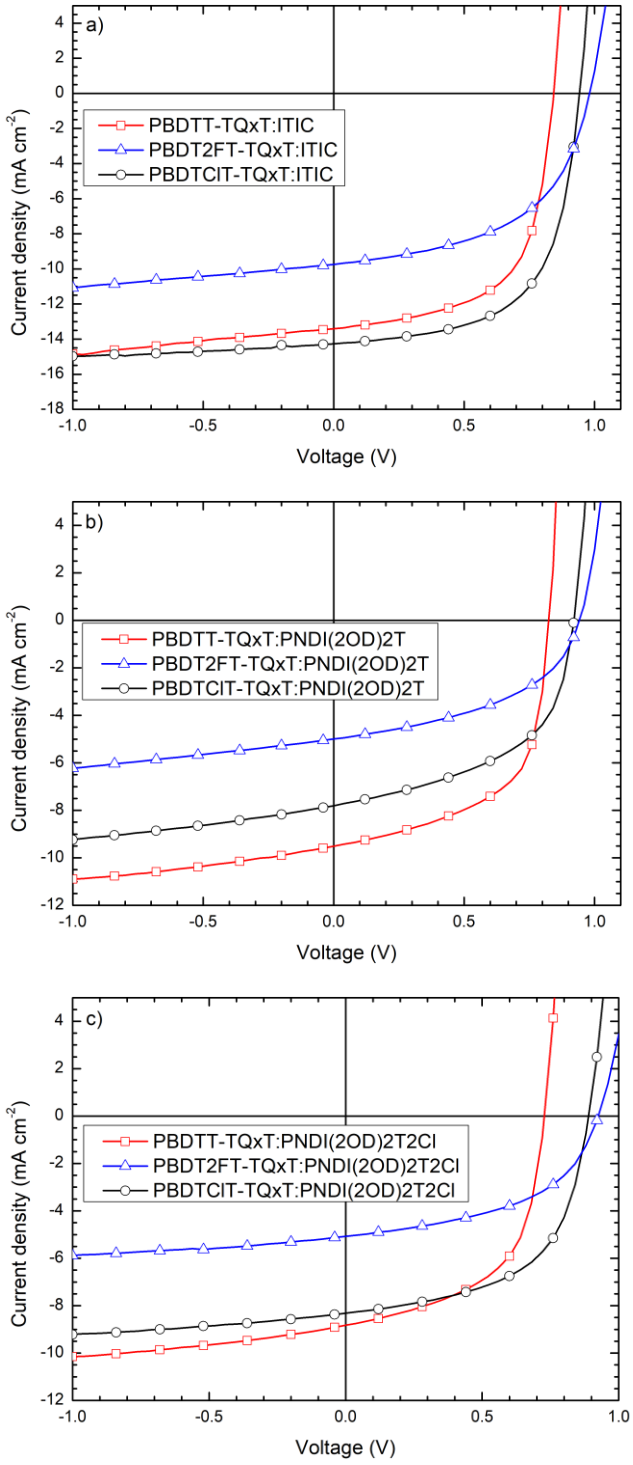

Figure 3. Current-density plots for the polymer solar cell devices (affording average PCEs) fabricated from the three donor polymers in combination with ITIC (a), PNDI(2OD)2T (b) and PNDI(2OD)2T2Cl (c).

Table 2. *J-V* parameters for the optimized polymer solar cells.

Donor:Acceptor	Additive (% DIO)	V_{OC} [a] (V)	J_{SC} [a] (mA cm^{-2})	FF [a]	PCE [a] (%)	Best PCE (%)
PBDTT-TQxT:ITIC [b]	1	0.84	13.57	0.65	7.39	7.45
PBDT2FT-TQxT:ITIC [b]	3	0.98	9.46	0.53	4.90	5.13
PBDTClT-TQxT:ITIC [b]	1	0.94	14.61	0.60	8.22	8.43
PBDTT-TQxT:PNDI(2OD)2T [b]	0.5	0.82	9.49	0.58	4.56	4.72
PBDT2FT-TQxT:PNDI(2OD)2T [b]	3	0.94	5.05	0.46	2.22	2.35
PBDTClT-TQxT:PNDI(2OD)2T [b]	1	0.92	7.87	0.53	3.81	3.97
PBDTT-TQxT:PNDI(2OD)2T2Cl [c]	0.5	0.73	8.58	0.57	3.54	3.88
PBDT2FT-TQxT:PNDI(2OD)2T2Cl [c]	3	0.92	4.91	0.54	2.43	2.84
PBDTClT-TQxT:PNDI(2OD)2T2Cl [c]	1	0.88	8.28	0.59	4.31	4.81

[a] Average values were taken over (at least) 4 devices. Inverted device architecture: glass/ITO/ZnO/active layer/MoO_x/Ag. Donor and acceptor were blended in a 1:1 weight ratio. [b] Total concentration of 20 mg mL^{-1} in chlorobenzene. [c] Total concentration of 16 mg mL^{-1} in chlorobenzene.

To get more insight into the observed variations of the *J-V* parameters, hole- and electron-only devices were made using a glass/ITO/PEDOT:PSS/active layer/MoO_x/Ag and glass/ITO/ZnO/active layer/Ca/Al architecture, respectively (**Table S4**, **Figure S20**). Whereas all mobility values are within the same range ($1 \cdot 10^{-5}$ to $5 \cdot 10^{-4}$ cm^{2}V^{-1}s^{-1}), the blends of the fluorinated donor polymer PBDT2FT-TQxT with the two acceptor polymers stand out because of their imbalanced hole and electron mobilities. AFM analysis of the active layers of all OPV devices was also performed and the resulting images are shown in **Figure 4**. Again, the most notable differences were observed for the blends based on the fluorinated donor polymer PBDT2FT-TQxT, showing a more rough surface, suggesting a higher degree of phase separation and thereby explaining the reduced J_{SC} observed for these devices.

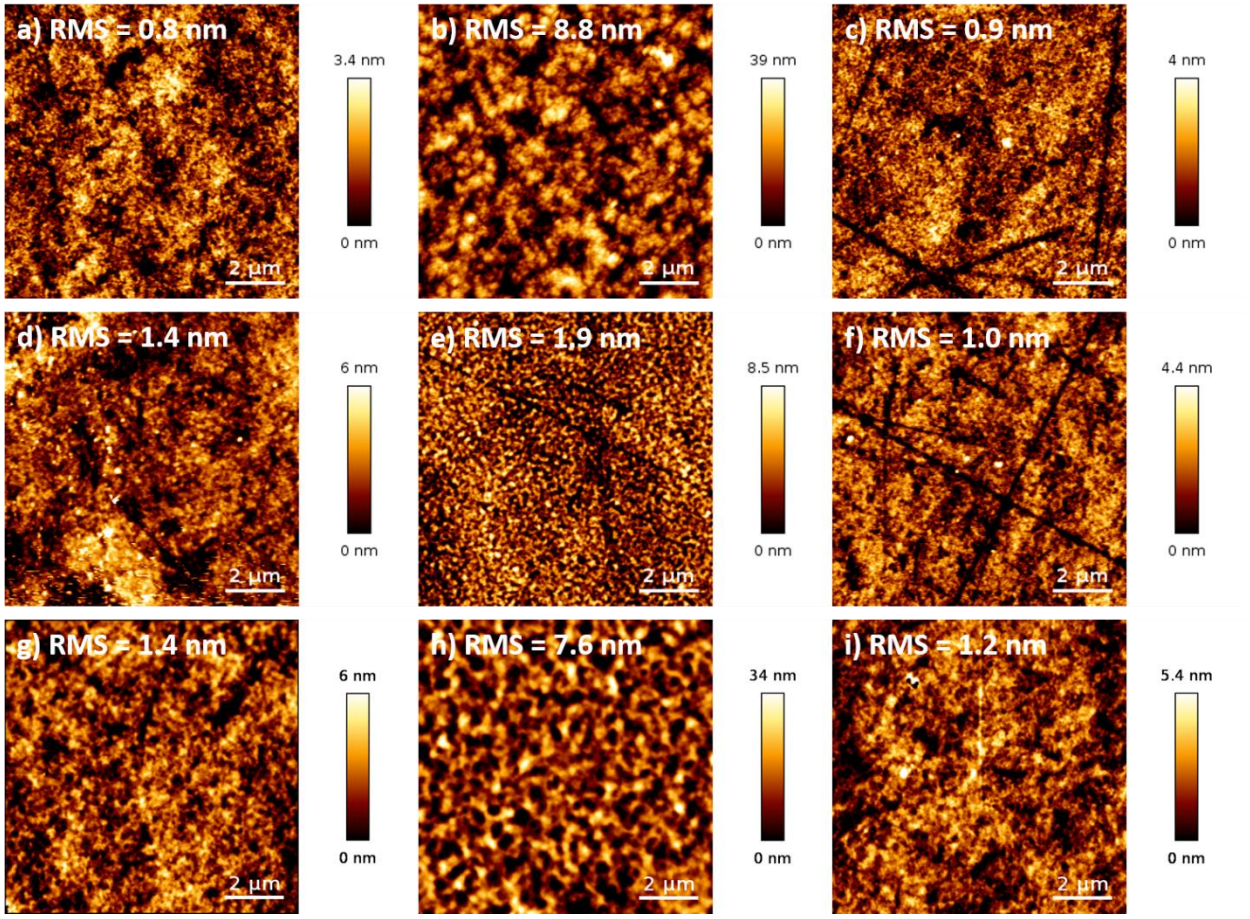

Figure 4. 10 x 10 µm AFM images obtained for polymer solar cell devices made from a) PBDTT-TQxT:ITIC, b) PBDT2FT-TQxT:ITIC, c) PBDTClT-TQxT:ITIC, d) PBDTT-TQxT:PNDI(2OD)2T, e) PBDT2FT-TQxT:PNDI(2OD)2T, f) PBDTClT-TQxT:PNDI(2OD)2T, g) PBDTT-TQxT:PNDI(2OD)2T2Cl, h) PBDT2FT-TQxT:PNDI(2OD)2T2Cl, and i) PBDTClT-TQxT:PNDI(2OD)2T2Cl.

Finally, external quantum efficiency (EQE) (**Figure S21**) and sensitive EQE (sEQE) (**Figure 5**) measurements were performed on all solar cell devices. Plotting the sensitively measured EQE spectra on a logarithmic scale reveals the presence of subgap absorption features for some of the donor:acceptor combinations. Using ITIC as acceptor results in the formation of a CT absorption band when combined with PBDTT-TQxT, which blue-shifts and disappears upon chlorination or fluorination of the donor (**Figure 5a**), as expected due to their lower HOMO energy levels. This indicates a reduction of the driving force for electron transfer to a value less than kT and results in an increase in V_{OC} (**Table 3**). A similar effect is observed when using PNDI(2OD)2T as acceptor (**Figure 5b**).

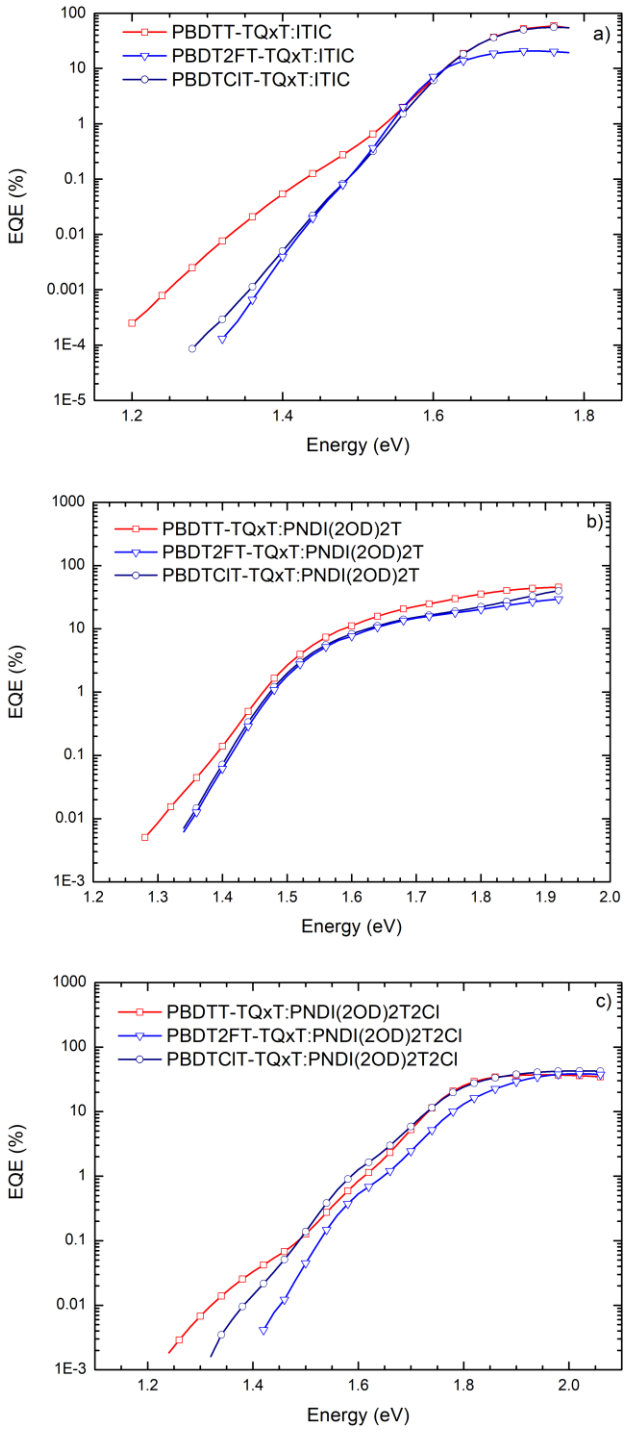

Figure 5. sEQE spectra for the polymer solar cell devices (affording average PCEs) fabricated from the three donor polymers in combination with ITIC (a), PNDI(2OD)2T (b) and PNDI(2OD)2T2Cl (c).

Also when using the chlorinated acceptor PNDI(2OD)2T2Cl, CT absorption bands are visible at photon energies < 1.4 eV, gradually blue-shifting with decreasing donor strength. Furthermore, a notable feature is apparent in the sEQE spectra at 1.6 eV for the devices with all three donor polymers. We

therefore attribute this feature to originate from the PNDI(2OD)2T2Cl polymer, as apparent from sEQE spectra of single layer PNDI(2OD)2T2Cl devices (**Figure S22**). This feature possibly originates from stacked PNDI(2OD)2T2Cl chains producing low energy interchain CT transitions[68] and is absent for the blends comprising regular PNDI(2OD)2T.

The theoretically maximum achievable V_{OC} under solar conditions, V_{OC}^{rad}, was calculated for every blend according to a previously reported method (**Table 3**).[69] Halogenation of the donor polymer results in an increase of the V_{OC}^{rad} with all three acceptors. The difference between the measured V_{OC} and V_{OC}^{rad} is due to non-radiative decay pathways only. The blends with the fluorinated donor exhibit the lowest V_{OC} loss ($\Delta V^{non\text{-}rad}$) with all three acceptors, resulting in the highest observed V_{OC} in OPV devices. Nevertheless, higher PCEs were obtained for blends of the non-halogenated and chlorinated polymers due to higher FF and J_{SC} values.

Table 3. Measured V_{OC}, calculated V_{OC}^{rad} and V_{OC} loss of the polymer solar cell devices.

Donor:Acceptor	**V_{OC} measured (V)**	**V_{OC}^{rad} calculated (V)**	**$\Delta V^{non\text{-}rad}$ (V)**
PBDTT-TQxT:ITIC	0.84	1.14	0.30
PBDT2FT-TQxT:ITIC	0.98	1.24	0.26
PBDTClT-TQxT:ITIC	0.94	1.24	0.30
PBDTT-TQxT:PNDI(2OD)2T	0.82	1.13	0.31
PBDT2FT-TQxT:PNDI(2OD)2T	0.94	1.16	0.22
PBDTClT-TQxT:PNDI(2OD)2T	0.92	1.16	0.24
PBDTT-TQxT:PNDI(2OD)2T2Cl	0.73	1.11	0.38
PBDT2FT-TQxT:PNDI(2OD)2T2Cl	0.92	1.21	0.29
PBDTClT-TQxT:PNDI(2OD)2T2Cl	0.88	1.21	0.33

Conclusions

Three donor copolymers based on 4,8-di(thiophen-2-yl)benzo[1,2-*b*:4,5-*b*']dithiophene were synthesized, varying the degree of halogenation of the thienyl substituents. Photovoltaic devices were made with either ITIC as small molecule acceptor or PNDI(2OD)2T and PNDI(2OD)2T2Cl as polymer acceptors. The chlorinated donor polymer PBDTClT-TQxT afforded the highest (average) efficiency of 8.2% in the ITIC series, which can mainly be attributed to the higher V_{OC} as compared to the non-halogenated donor polymer. For PNDI(2OD)2T, the higher V_{OC} obtained with the chlorinated donor polymer did not compensate for the lower FF and J_{SC}. As a result, the non-halogenated PBDTT-TQxT donor polymer worked best with the non-halogenated acceptor polymer, achieving a PCE of 4.6%. When combined with the chlorinated acceptor polymer PNDI(2OD)2T2Cl, the chlorinated donor again afforded

the best result, with a PCE of 4.3%. Although the PBDT2FT-TQxT blends gave the highest V_{OC} values, up to 0.98 V with ITIC, and the lowest V_{OC} losses with all three electron acceptors, this donor polymer always afforded the lowest efficiencies. The severely lowered J_{SC} and FF values are likely related to unfavorable interactions of the fluorinated copolymer with the acceptor materials. As the PBDTClT-TQxT donor polymer clearly gave the most promising results and is also much easier to synthesize as compared to the fluorinated derivative, we conclude that chlorination is an undervalued approach to afford high-performance OPV materials and blends and should receive more attention by the organic electronics community.

Acknowledgements

This work is supported by the Research Foundation – Flanders (FWO Vlaanderen) (projects G.0B67.15N, G0B2718N and G0D0118N, and Hercules project GOH3816NAUHL). P. Verstappen is a postdoctoral fellow of the FWO Vlaanderen. The authors like to thank H. Penxten for the CV measurements.

Supplementary data

Additional details on the experimental methods, synthetic procedures, gel permeation chromatograms, cyclic voltammograms, ^{1}H NMR spectra of the monomers, MALDI-ToF mass spectra, optimized geometries and HOMO/LUMO topologies, photovoltaic device fabrication and characterization, hole- and electron-only devices and (s)EQE measurements.

References

1. Ma, R.; Liu, T.; Luo, Z.; Guo, Q.; Xiao, Y.; Chen, Y.; Li, X.; Luo, S.; Lu, X.; Zhang, M.; Li, Y.; Yan, H., Improving open-circuit voltage by a chlorinated polymer donor endows binary organic solar cells efficiencies over 17%. *Sci. Chin. Chem.* **2020**, *63*, 325-330.
2. Fan, B.; Ying, L.; Wang, Z.; He, B.; Jiang, X.-F.; Huang, F.; Cao, Y., Optimisation of processing solvent and molecular weight for the production of green-solvent-processed all-polymer solar cells with a power conversion efficiency over 9%. *Energy Environ. Sci.* **2017,** *10* (5), 1243-1251.
3. Yan, C.; Barlow, S.; Wang, Z.; Yan, H.; Jen, A. K. Y.; Marder, S. R.; Zhan, X., Non-fullerene acceptors for organic solar cells. *Nat. Rev. Mater.* **2018,** *3* (3), 18003.
4. Kim, T.; Younts, R.; Lee, W.; Lee, S.; Gundogdu, K.; Kim, B. J., Impact of the photo-induced degradation of electron acceptors on the photophysics, charge transport and device performance of all-polymer and fullerene–polymer solar cells. *J. Mater. Chem. A* **2017,** *5* (42), 22170-22179.
5. Kim, T.; Choi, J.; Kim, H. J.; Lee, W.; Kim, B. J., Comparative Study of Thermal Stability, Morphology, and Performance of All-Polymer, Fullerene–Polymer, and Ternary Blend Solar Cells Based on the Same Polymer Donor. *Macromolecules* **2017,** *50* (17), 6861-6871.
6. Zhao, W.; Qian, D.; Zhang, S.; Li, S.; Inganas, O.; Gao, F.; Hou, J., Fullerene-Free Polymer Solar Cells with over 11% Efficiency and Excellent Thermal Stability. *Adv. Mater.* **2016,** *28* (23), 4734-4739.
7. Yuan, J.; Zhang, Y.; Zhou, L.; Zhang, G.; Yip, H.-L.; Lau, T.-K.; Lu, X.; Zhu, C.; Peng, H.; Johnson, P. A.; Leclerc, M.; Cao, Y.; Ulanski, J.; Li, Y.; Zou, Y., Single-Junction Organic Solar Cell with over 15% Efficiency Using Fused-Ring Acceptor with Electron-Deficient Core. *Joule* **2019,** *3* (4), 1140-1151.

8. Li, Z.; Ying, L.; Zhu, P.; Zhong, W.; Li, N.; Liu, F.; Huang, F.; Cao, Y., A generic green solvent concept boosting the power conversion efficiency of all-polymer solar cells to 11%. *Energy & Environmental Science* **2019,** *12* (1), 157-163.
9. Yao, H.; Bai, F.; Hu, H.; Arunagiri, L.; Zhang, J.; Chen, Y.; Yu, H.; Chen, S.; Liu, T.; Lai, J. Y. L.; Zou, Y.; Ade, H.; Yan, H., Efficient All-Polymer Solar Cells based on a New Polymer Acceptor Achieving 10.3% Power Conversion Efficiency. *ACS Energy Lett.* **2019,** *4* (2), 417-422.
10. Lizin, S.; Van Passel, S.; De Schepper, E.; Maes, W.; Lutsen, L.; Manca, J.; Vanderzande, D., Life cycle analyses of organic photovoltaics: a review. *Energy Environ. Sci.* **2013,** *6* (11), 3136-3149.
11. Cardinaletti, I.; Kesters, J.; Bertho, S.; Conings, B.; Piersimoni, F.; D'Haen, J.; Lutsen, L.; Nesladek, M.; Van Mele, B.; Van Assche, G.; Vandewal, K.; Salleo, A.; Vanderzande, D.; Maes, W.; Manca, J. V., Toward bulk heterojunction polymer solar cells with thermally stable active layer morphology. *J. Photonics Energy* **2014,** *4* (1), 040997.
12. Baran, D.; Ashraf, R. S.; Hanifi, D. A.; Abdelsamie, M.; Gasparini, N.; Rohr, J. A.; Holliday, S.; Wadsworth, A.; Lockett, S.; Neophytou, M.; Emmott, C. J.; Nelson, J.; Brabec, C. J.; Amassian, A.; Salleo, A.; Kirchartz, T.; Durrant, J. R.; McCulloch, I., Reducing the efficiency-stability-cost gap of organic photovoltaics with highly efficient and stable small molecule acceptor ternary solar cells. *Nat. Mater.* **2017,** *16* (3), 363-369.
13. Cheng, P.; Bai, H.; Zawacka, N. K.; Andersen, T. R.; Liu, W.; Bundgaard, E.; Jorgensen, M.; Chen, H.; Krebs, F. C.; Zhan, X., Roll-Coated Fabrication of Fullerene-Free Organic Solar Cells with Improved Stability. *Adv. Sci.* **2015,** *2* (6), 1500096.
14. Liu, Q.; Jiang, Y.; Jin, K.; Qin, J.; Xu, J.; Li, W.; Xiong, J.; Liu, J.; Xiao, Z.; Sun, K.; Yang, S.; Zhang, X.; Ding, L., 18% Efficiency organic solar cells. *Sci. Bull.* **2020,** *65*, 272-275.
15. Meng, Y.; Wu, J.; Guo, X.; Su, W.; Zhu, L.; Fang, J.; Zhang, Z.-G.; Liu, F.; Zhang, M.; Russell, T. P.; Li, Y., 11.2% Efficiency all-polymer solar cells with high open-circuit voltage. *Sci. Chin. Chem.* **2019,** *62* (7), 845-850.
16. Zhu, L.; Zhong, W.; Qiu, C.; Lyu, B.; Zhou, Z.; Zhang, M.; Song, J.; Xu, J.; Wang, J.; Ali, J.; Feng, W.; Shi, Z.; Gu, X.; Ying, L.; Zhang, Y.; Liu, F., Aggregation-Induced Multilength Scaled Morphology Enabling 11.76% Efficiency in All-Polymer Solar Cells Using Printing Fabrication. *Adv. Mater.* **2019,** *31*, 1902899.
17. Li, Z.; Zhong, W.; Ying, L.; Liu, F.; Li, N.; Huang, F.; Cao, Y., Morphology optimization via molecular weight tuning of donor polymer enables all-polymer solar cells with simultaneously improved performance and stability. *Nano Energy* **2019,** *64*, 103931.
18. Zhang, Y.; Xu, Y.; Ford, M. J.; Li, F.; Sun, J.; Ling, X.; Wang, Y.; Gu, J.; Yuan, J.; Ma, W., Thermally Stable All-Polymer Solar Cells with High Tolerance on Blend Ratios. *Adv. Energy Mater.* **2018**, 1800029.
19. Kim, T.; Kim, J. H.; Kang, T. E.; Lee, C.; Kang, H.; Shin, M.; Wang, C.; Ma, B.; Jeong, U.; Kim, T. S.; Kim, B. J., Flexible, highly efficient all-polymer solar cells. *Nat. Commun.* **2015,** *6*, 8547.
20. Yao, H.; Ye, L.; Zhang, H.; Li, S.; Zhang, S.; Hou, J., Molecular Design of Benzodithiophene-Based Organic Photovoltaic Materials. *Chem. Rev.* **2016,** *116* (12), 7397-457.
21. Holliday, S.; Li, Y. L.; Luscombe, C. K., Recent advances in high performance donor-acceptor polymers for organic photovoltaics. *Prog. Polym. Sci.* **2017,** *70*, 34-51.
22. Lee, C.; Giridhar, T.; Choi, J.; Kim, S.; Kim, Y.; Kim, T.; Lee, W.; Cho, H.-H.; Wang, C.; Ade, H.; Kim, B. J., Importance of 2D Conjugated Side Chains of Benzodithiophene-Based Polymers in Controlling Polymer Packing, Interfacial Ordering, and Composition Variations of All-Polymer Solar Cells. *Chem. Mater.* **2017,** *29* (21), 9407-9415.
23. Gu, C.; Liu, D.; Wang, J.; Niu, Q.; Gu, C.; Shahid, B.; Yu, B.; Cong, H.; Yang, R., Alkylthienyl substituted asymmetric 2D BDT and DTBT-based polymer solar cells with a power conversion efficiency of 9.2%. *J. Mater. Chem. A* **2018,** *6* (5), 2371-2378.

24. Xiao, B.; Tang, A.; Yang, J.; Mahmood, A.; Sun, X.; Zhou, E., Quinoxaline-Containing Nonfullerene Small-Molecule Acceptors with a Linear A_2-A_1-D-A_1-A_2 Skeleton for Poly(3-hexylthiophene)-Based Organic Solar Cells. *ACS Appl. Mater. Interfaces* **2018,** *10* (12), 10254-10261.
25. Yang, J.; Cong, P.; Chen, L.; Wang, X.; Li, J.; Tang, A.; Zhang, B.; Geng, Y.; Zhou, E., Introducing Fluorine and Sulfur Atoms into Quinoxaline-Based p-type Polymers To Gradually Improve the Performance of Fullerene-Free Organic Solar Cells. *ACS Macro Lett.* **2019,** *8*, 743-748.
26. Xiao, B.; Zhang, Q.; Li, G.; Du, M.; Geng, Y.; Sun, X.; Tang, A.; Liu, Y.; Guo, Q.; Zhou, E., Side chain engineering of quinoxaline-based small molecular nonfullerene acceptors for high-performance poly(3-hexylthiophene)-based organic solar cells. *Sci. Chin. Chem.* **2020,** *63* (2), 254-264.
27. Gedefaw, D.; Prosa, M.; Bolognesi, M.; Seri, M.; Andersson, M. R., Recent Development of Quinoxaline Based Polymers/Small Molecules for Organic Photovoltaics. *Adv. Energy Mater.* **2017,** *7* (21), 1700575.
28. Verstappen, P.; Kesters, J.; D'Olieslaeger, L.; Drijkoningen, J.; Cardinaletti, I.; Vangerven, T.; Bruijnaers, B. J.; Willems, R. E. M.; D'Haen, J.; Manca, J. V.; Lutsen, L.; Vanderzande, D. J. M.; Maes, W., Simultaneous Enhancement of Solar Cell Efficiency and Stability by Reducing the Side Chain Density on Fluorinated PCPDTQx Copolymers. *Macromolecules* **2015,** *48* (12), 3873-3882.
29. Meyer, F., Fluorinated conjugated polymers in organic bulk heterojunction photovoltaic solar cells. *Prog. Polym. Sci.* **2015,** *47*, 70-91.
30. Leclerc, N.; Chávez, P.; Ibraikulov, O.; Heiser, T.; Lévêque, P., Impact of Backbone Fluorination on π-Conjugated Polymers in Organic Photovoltaic Devices: A Review. *Polymers* **2016,** *8* (1), 11.
31. Ibraikulov, O. A.; Ngov, C.; Chávez, P.; Bulut, I.; Heinrich, B.; Boyron, O.; Gerasimov, K. L.; Ivanov, D. A.; Swaraj, S.; Méry, S.; Leclerc, N.; Lévêque, P.; Heiser, T., Face-on orientation of fluorinated polymers conveyed by long alkyl chains: a prerequisite for high photovoltaic performances. *J. Mater. Chem. A* **2018,** *6* (25), 12038-12045.
32. Verstappen, P.; Kesters, J.; Vanormelingen, W.; Heintges, G. H. L.; Drijkoningen, J.; Vangerven, T.; Marin, L.; Koudjina, S.; Champagne, B.; Manca, J.; Lutsen, L.; Vanderzande, D.; Maes, W., Fluorination as an effective tool to increase the open-circuit voltage and charge carrier mobility of organic solar cells based on poly(cyclopenta[2,1-b:3,4-b']dithiophene-alt-quinoxaline) copolymers. *J. Mater. Chem. A* **2015,** *3* (6), 2960-2970.
33. Jung, J. W.; Jo, J. W.; Chueh, C. C.; Liu, F.; Jo, W. H.; Russell, T. P.; Jen, A. K., Fluoro-Substituted n-Type Conjugated Polymers for Additive-Free All-Polymer Bulk Heterojunction Solar Cells with High Power Conversion Efficiency of 6.71. *Adv. Mater.* **2015,** *27* (21), 3310-3317.
34. Liu, Z.; Gao, Y.; Dong, J.; Yang, M.; Liu, M.; Wen, J.; Zhang, Y.; Ma, H.; Gao, X.; Chen, W.; Shao, M., Chlorinated Wide Bandgap Donor Polymer Enabling Annealing Free Non-Fullerene Solar Cells with the Efficiency of 11.5. *J. Phys. Chem. Lett.* **2018,** *9*, 6955-6962.
35. Zhang, S.; Qin, Y.; Zhu, J.; Hou, J., Over 14% Efficiency in Polymer Solar Cells Enabled by a Chlorinated Polymer Donor. *Adv. Mater.* **2018,** *30* (20), e1800868.
36. Jeon, S. J.; Han, Y. W.; Moon, D. K., Chlorine Effects of Heterocyclic Ring-Based Donor Polymer for Low-Cost and High-Performance Nonfullerene Polymer Solar Cells. *Solar RRL* **2019**, 1900094.
37. Zhang, H.; Yao, H.; Hou, J.; Zhu, J.; Zhang, J.; Li, W.; Yu, R.; Gao, B.; Zhang, S.; Hou, J., Over 14% Efficiency in Organic Solar Cells Enabled by Chlorinated Nonfullerene Small-Molecule Acceptors. *Adv. Mater.* **2018,** *30* (28), e1800613.
38. Zhang, Y. B.; Gao, X.; Li, J. L.; Tu, G. L., Highly selective Palladium-catalyzed Suzuki coupling reaction toward chlorine-containing electroluminescence polymers. *Dyes Pigm.* **2015,** *120*, 112-117.
39. Chen, H.-C.; Chen, Y.-H.; Liu, C.-C.; Chien, Y.-C.; Chou, S.-W.; Chou, P.-T., Prominent Short-Circuit Currents of Fluorinated Quinoxaline-Based Copolymer Solar Cells with a Power Conversion Efficiency of 8.0%. *Chem. Mater.* **2012,** *24* (24), 4766-4772.
40. Liu, D.; Zhao, W.; Zhang, S.; Ye, L.; Zheng, Z.; Cui, Y.; Chen, Y.; Hou, J., Highly Efficient Photovoltaic

Polymers Based on Benzodithiophene and Quinoxaline with Deeper HOMO Levels. *Macromolecules* **2015,** *48* (15), 5172-5178.
41. Zhao, Z.; Zhang, Y.; Wang, Y.; Qin, X.; Wu, J.; Hou, J., Fluorinated and non-fluorinated conjugated polymers showing different photovoltaic properties in polymer solar cells with PFNBr interlayers. *Org. Electron.* **2016,** *28*, 178-183.
42. Zheng, Z.; Awartani, O. M.; Gautam, B.; Liu, D.; Qin, Y.; Li, W.; Bataller, A.; Gundogdu, K.; Ade, H.; Hou, J., Efficient Charge Transfer and Fine-Tuned Energy Level Alignment in a THF-Processed Fullerene-Free Organic Solar Cell with 11.3% Efficiency. *Adv. Mater.* **2017,** *29* (5), 1604241.
43. Xu, S. T.; Wang, X. J.; Feng, L. L.; He, Z. C.; Peng, H. J.; Cimrova, V.; Yuan, J.; Zhang, Z. G.; Li, Y. F.; Zou, Y. P., Optimizing the conjugated side chains of quinoxaline based polymers for nonfullerene solar cells with 10.5% efficiency. *J. Mater. Chem. A* **2018,** *6* (7), 3074-3083.
44. Xu, S.; Feng, L.; Yuan, J.; Zhang, Z. G.; Li, Y.; Peng, H.; Zou, Y., Hexafluoroquinoxaline Based Polymer for Nonfullerene Solar Cells Reaching 9.4% Efficiency. *ACS Appl. Mater. Interfaces* **2017,** *9* (22), 18816-18825.
45. Zhang, Z. Z.; Feng, L. L.; Xu, S. T.; Yuan, J.; Zhang, Z. G.; Peng, H. J.; Li, Y. F.; Zou, Y. P., Achieving over 10% efficiency in a new acceptor ITTC and its blends with hexafluoroquinoxaline based polymers. *J. Mater. Chem. A* **2017,** *5* (22), 11286-11293.
46. Chen, X.; Zhao, M.; Zhang, Z.-G.; Li, Y.; Li, X.; Wang, H., High-Efficiency All Polymer Solar Cell with a Low Voltage Loss of 0.56 V. *ACS Appl. Energy Mater.* **2018,** *1* (5), 2350-2357.
47. Cui, Y.; Yao, H.; Zhang, J.; Zhang, T.; Wang, Y.; Hong, L.; Xian, K.; Xu, B.; Zhang, S.; Peng, J.; Wei, Z.; Gao, F.; Hou, J., Over 16% efficiency organic photovoltaic cells enabled by a chlorinated acceptor with increased open-circuit voltages. *Nat. Commun.* **2019,** *10*, 2515.
48. Wang, C.-K.; Jiang, B.-H.; Lu, J.-H.; Cheng, M.-T.; Jeng, R.-J.; Lu, Y.-W.; Chen, C.-P.; Wong, K.-T., A Near-Infrared Absorption Small Molecule Acceptor for High-Performance Semitransparent and Colorful Binary and Ternary Organic Photovoltaics. *ChemSusChem* **2020,** *13*, 903-913.
49. Meng, H.; Li, Y.; Pang, B.; Li, Y.; Xiang, Y.; Guo, L.; Li, X.; Zhan, C.; Huang, J., Effects of Halogenation in B ← N Embedded Polymer Acceptors on Performance of All-Polymer Solar Cells. *ACS Appl. Mater. Interfaces* **2020,** *12*, 2733-2742.
50. Luo, Z.; Liu, T.; Wang, Y.; Zhang, G.; Sun, R.; Chen, Z.; Zhong, C.; Wu, J.; Chen, Y.; Zhang, M.; Zou, Y.; Ma, W.; Yan, H.; Min, J.; Li, Y.; Yang, C., Reduced Energy Loss Enabled by a Chlorinated Thiophene-Fused Ending-Group Small Molecular Acceptor for Efficient Nonfullerene Organic Solar Cells with 13.6% Efficiency. *Adv. Energy Mater.* **2019,** *9* (18), 1900041.
51. Ryu, G.-S.; Chen, Z.; Usta, H.; Noh, Y.-Y.; Facchetti, A., Naphthalene diimide-based polymeric semiconductors. Effect of chlorine incorporation and n-channel transistors operating in water. *MRS Commun.* **2016,** *6* (1), 47-60.
52. Dey, S., Recent Progress in Molecular Design of Fused Ring Electron Acceptors for Organic Solar Cells. *Small* **2019**, e1900134.
53. Bauer, N.; Zhang, Q.; Rech, J. J.; Dai, S.; Peng, Z.; Ade, H.; Wang, J.; Zhan, X.; You, W., The impact of fluorination on both donor polymer and non-fullerene acceptor: The more fluorine, the merrier. *Nano Res.* **2019**, *12*, 2400-2405.
54. Xue, L.; Yang, Y.; Xu, J.; Zhang, C.; Bin, H.; Zhang, Z. G.; Qiu, B.; Li, X.; Sun, C.; Gao, L.; Yao, J.; Chen, X.; Yang, Y.; Xiao, M.; Li, Y., Side Chain Engineering on Medium Bandgap Copolymers to Suppress Triplet Formation for High-Efficiency Polymer Solar Cells. *Adv. Mater.* **2017,** *29*, 1703344.
55. Cho, S.-N.; Lee, W.-H.; Park, J. B.; Kim, J.-H.; Hwang, D.-H.; Kang, I.-N., Synthesis and characterization of fluorine atom substituted new BDT-based polymers for use in organic solar cells. *Synth. Met.* **2015,** *210*, 273-281.
56. Hou, J.; Park, M.-H.; Zhang, S.; Yao, Y.; Chen, L.-M.; Li, J.-H.; Yang, Y., Bandgap and Molecular Energy Level Control of Conjugated Polymer Photovoltaic Materials Based on Benzo[1,2-b:4,5-

b']dithiophene. *Macromolecules* **2008,** *41* (16), 6012-6018.
57. Huo, L.; Hou, J.; Zhang, S.; Chen, H. Y.; Yang, Y., A polybenzo[1,2-b:4,5-b']dithiophene derivative with deep HOMO level and its application in high-performance polymer solar cells. *Angew. Chem. Int. Ed.* **2010,** *49* (8), 1500-1503.
58. Yan, H.; Chen, Z.; Zheng, Y.; Newman, C.; Quinn, J. R.; Dotz, F.; Kastler, M.; Facchetti, A., A high-mobility electron-transporting polymer for printed transistors. *Nature* **2009,** *457* (7230), 679-686.
59. Lin, Z.; Liu, X.; Zhang, W.; Wei, C.; Huang, J.; Chen, Z.; Wang, L.; Yu, G., Regioirregular ambipolar naphthalenediimide-based alternating polymers: Synthesis, characterization, and application in field-effect transistors. *J. Polym. Sci. A: Polym. Chem.* **2017,** *55* (21), 3627-3635.
60. Hendsbee, A. D.; McAfee, S. M.; Sun, J.-P.; McCormick, T. M.; Hill, I. G.; Welch, G. C., Phthalimide-based π-conjugated small molecules with tailored electronic energy levels for use as acceptors in organic solar cells. *J. Mater. Chem. C* **2015,** *3* (34), 8904-8915.
61. Kim, J.; Baek Park, J.; Lee, W.-H.; Kim, J.-H.; Hwang, D.-H.; Kang, I.-N., High-performance fluorine-containing BDT-based copolymer for organic solar cells with a high open circuit voltage. *J. Polym. Sci. A: Polym. Chem.* **2017,** *55* (15), 2506-2512.
62. Po, R.; Bianchi, G.; Carbonera, C.; Pellegrino, A., "All That Glisters Is Not Gold": An Analysis of the Synthetic Complexity of Efficient Polymer Donors for Polymer Solar Cells. *Macromolecules* **2015,** *48* (3), 453-461.
63. Vangerven, T.; Verstappen, P.; Patil, N.; D'Haen, J.; Cardinaletti, I.; Benduhn, J.; Van den Brande, N.; Defour, M.; Lemaur, V.; Beljonne, D.; Lazzaroni, R.; Champagne, B.; Vandewal, K.; Andreasen, J. W.; Adriaensens, P.; Breiby, D. W.; Van Mele, B.; Vanderzande, D.; Maes, W.; Manca, J., Elucidating Batch-to-Batch Variation Caused by Homocoupled Side Products in Solution-Processable Organic Solar Cells. *Chem. Mater.* **2016,** *28* (24), 9088-9098.
64. Pirotte, G.; Verstappen, P.; Vanderzande, D.; Maes, W., On the "True" Structure of Push-Pull-Type Low-Bandgap Polymers for Organic Electronics. *Adv. Electron. Mater.* **2018,** *4* (10), 1700481.
65. Xu, X.; Li, Z.; Wang, J.; Lin, B.; Ma, W.; Xia, Y.; Andersson, M. R.; Janssen, R. A. J.; Wang, E., High-performance all-polymer solar cells based on fluorinated naphthalene diimide acceptor polymers with fine-tuned crystallinity and enhanced dielectric constants. *Nano Energy* **2018**, *45*, 368-379.
66. Gaussian 16, Revision A.03, Frisch, M. J.; Trucks, G. W.; Schlegel, H. B.; Scuseria, G. E.; Robb, M. A.; Cheeseman, J. R.; Scalmani, G.; Barone, V.; Petersson, G. A.; Nakatsuji, H.; Li, X.; Caricato, M.; Marenich, A. V.; Bloino, J.; Janesko, B. G.; Gomperts, R.; Mennucci, B.; Hratchian, H. P.; Ortiz, J. V.; Izmaylov, A. F.; Sonnenberg, J. L.; Williams-Young, D.; Ding, F.; Lipparini, F., Egidi, F.; Goings, J.; Peng, B.; Petrone, A.; Henderson, T.; Ranasinghe, D.; Zakrzewski, V. G.; Gao, J.; Rega, N.; Zheng, G.; Liang, W.; Hada, M.; Ehara, M.; Toyota, K.; Fukuda, R.; Hasegawa, J.; Ishida, M.; Nakajima, T.; Honda, Y.; Kitao, O.; Nakai, H.; Vreven, T.; Throssell, K.; Montgomery, Jr., J. A.; Peralta, J. E.; Ogliaro, F.; Bearpark, M. J.; Heyd, J. J.; Brothers, E. N.; Kudin, K. N.; Staroverov, V. N.; Keith, T. A.; Kobayashi, R.; Normand, J.; Raghavachari, K.; Rendell, A. P.; Burant, J. C.; Iyengar, S. S.; Tomasi, J.; Cossi, M.; Millam, J. M.; Klene, M.; Adamo, C.; Cammi, R.; Ochterski, J. W.; Martin, R. L.; Morokuma, K.; Farkas, O.; Foresman, J. B.; Fox, D. J., Gaussian, Inc., Wallingford CT, 2016.
67. Zhao, Y.; Truhlar, D. G., The M06 suite of density functionals for main group thermochemistry, thermochemical kinetics, noncovalent interactions, excited states, and transition elements: two new functionals and systematic testing of four M06-class functionals and 12 other functionals. *Theor. Chem. Acc.* **2008,** *120*, 215-241.
68. Steyrleuthner, R.; Schubert, M.; Howard, I.; Klaumunzer, B.; Schilling, K.; Chen, Z.; Saalfrank, P.; Laquai, F.; Facchetti, A.; Neher, D., Aggregation in a high-mobility n-type low-bandgap copolymer with implications on semicrystalline morphology. *J. Am. Chem. Soc.* **2012,** *134* (44), 18303-18317.
69. Vandewal, K.; Tvingstedt, K.; Gadisa, A.; Inganas, O.; Manca, J. V., On the origin of the open-circuit voltage of polymer-fullerene solar cells. *Nat. Mater.* **2009**, *8* (11), 904-909.